NASA Technical Memorandum 83417
AIAA-83-1389

The Performance and Application of High Speed Long Life LH_2 Hybrid Bearings for Reusable Rocket Engine Turbomachinery

N. P. Hannum
Lewis Research Center
Cleveland, Ohio

and

C. E. Nielson
Rockwell International
Rocketdyne Division
Canoga Park, California

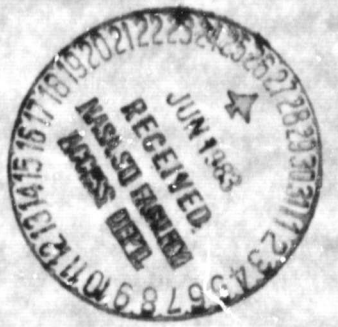

Prepared for the
Nineteenth Joint Propulsion Conference
cosponsored by the AIAA, SAE, and ASME
Seattle, Washington, June 27-29, 1983

THE PERFORMANCE AND APPLICATION OF HIGH SPEED LONG LIFE LH_2 HYBRID BEARINGS FOR REUSABLE ROCKET ENGINE TURBOMACHINERY

N. P. Hannum
National Aeronautics and Space Administration
Lewis Research Center
Cleveland, Ohio

and

C. E. Nielson
Rockwell International
Rocketdyne Division
Canoga Park, CA

ABSTRACT

Data are presented for two different experimental programs which were conducted to investigate the characteristics of a hybrid (hydrostatic/ball) bearing operating in liquid hydrogen. The same bearing design was used in both programs. Analytical predictions were made of the bearing characteristics and are compared with the experimental results when possible. The first program used a bearing tester to determine the steady state, transient, and cyclic life characteristics of the bearing over a wide range of operating conditions. The second program demonstrated the feasibility of applying hybrid bearings to an actual high speed turbopump by retrofitting and then testing an existing liquid hydrogen turbopump with the bearings.

E-1707

SYMBOLS

C radial clearance

D journal diameter

DPF $(P_p - P_a)$ film pressure drop

DPT $(P_s - P_a)$ total pressure drop

FLOR measured flow rate - predicted flow rate

K direct stiffness

K dimensionless stiffness $((Kc) - ((P_s - P_a)LD))$

L journal length

P pressure

PR DPF - DPT pressure ratio

Subscripts

p pocket

a sump

s supply

INTRODUCTION

The evolution of cryogenic turbopumps to support fully reusable chemical rocket propulsion has placed new demands on bearings. New bearing technology is needed to significantly increase service life and to increase the damping characteristics to meet these demands. In addition, the precision of the analytical models for stiffness and damping must be improved so that accurate predictions can be made for the complex dynamics of contemporary multiple stage, high speed, lightweight, cryogenic turbopumps.

Actual test experience with conventional ball bearings in the Space Shuttle Main Engine turbopumps has confirmed the analytical predictions that bearing life is far short of the reusability goals. Order-of-magnitude improvement in life is required. Some improvement may come through the use of better materials, but large improvements in life for rolling element bearings requires either reducing the bearing speed or the bearing load. Hybrid bearing systems consisting of both hydrostatic film and conventional ball bearings can accomplish both of these requirements plus add considerable damping to the rotor assembly.

In 1974, following the decision to develop a Space Shuttle and a fully reusable space transportation system, the Lewis Research Center initiated a systematic program to investigate hybrid bearings. Lewis contracted with Mechanical Technologies Incorporated to design and fabricate hybrid bearings with a 20 mm bore for use at speeds up to 12 600 rad/s (120 000 rpm). The size and operating conditions were selected to be compatible with the bearing requirements of an advanced technology turbopump being designed and fabricated by Rocketdyne Division of Rockwell International on another Lewis technology contract. The hybrid bearing designs used results from a 1967 U.S. Air Force contract with Pratt & Whitney Aircraft Incorporated. In the Lewis program, the hybrid bearing was first tested under simulated pump conditions in a cryogenic bearing tester to experimentally verify the design and operating characteristics. The bearing was then installed in a small LH_2 high technology turbopump to determine the operating characteristics in an actual pump environment.

The objectives of the hybrid bearing experimental programs were to (1) characterize the steady state operation in simulated LH_2 turbopump environments, (2) evaluate the life characteristics with cyclic tests, (3) determine integration requirements by retrofitting an existing LH_2 turbopump, (4) verify and/or improve the analytical models, and (5) demonstrate the feasibility of using a hybrid bearing in a high speed cryogenic turbopump.

Analytical predictions were made of the hybrid bearing characteristics and are compared with experimental results. A bearing tester was used to determine the steady state, transient, and cyclic life characteristics of the hybrid bearing over a wide range of operating conditions. An existing high speed turbopump was used as a test bed to determine experimentally the integration requirements and to demonstrate the feasibility of hybrid bearings.

APPARATUS

The experimental investigation of hybrid bearings was conducted jointly at the NASA Lewis Research Center and under contract at Rocketdyne Division of Rockwell International. The NASA testing used a specially designed bearing tester to simulate the LH_2 pump environment. The Rocketdyne testing used a MK48 liquid hydrogen turbopump.

Hybrid Bearings

The hybrid bearings consisted of two angular contact ball bearings installed in duplex fashion in a rotating cartridge. This cartridge was the rotating, or journal, component of the hydrostatic bearing and was separated from the stationary fluid film bearing at the outside diameter by a high tolerance clearance. A schematic of the hybrid bearing and photographs of the various components is shown in Figure 1. The ball bearings were preloaded against one another and separated by belleville spring washers which were capable of providing preloads of 111 to 666 N (25 to 150 lb). Liquid hydrogen was supplied to the bearing through two rows of 10 pockets each equally spaced around the fluid film bearing circumference. Dimensions for hydrostatic and ball bearings are shown in Tables 1 and 2.

NASA Bearing Tester

The NASA bearing tester was used to determine both the steady state and the transient operating characteristics of the hybrid bearing. The bearing tester consisted of a horizontal shaft supported at both ends by test bearings (Fig. 2(a)). The shaft was driven by a turbine. Axial shaft loads were supported by a hydrostatic thrust bearing. Experimental radial shaft loads were applied by a radial loading device. This device consisted of a hydrostatic bearing acting over a 60° arc of a cylindrical surface located at the mid span between the bearings. Applied loads were developed by the hydrostatic pressure acting over the area of the bearing "foot" and were shared equally by both test bearings. The turbine was driven by ambient temperature hydrogen gas to design speeds of up to 12 600 rad/s (120 000 rpm) and could deliver up to 12 kW (16.2 hp). Sufficient torque was developed to accelerate the shaft at up to 5200 rad/s^2 (50 000 rpm/s). Liquid hydrogen was supplied independently to each of the test bearings through passages in the housing and was drained from the tester through a common drain. Closed loop controllers were used to independently control the radial load, the drain pressure and the bearing supply pressures to either set points or as functions of speed.

MK48 Turbopump

The MK48 turbopump, a high speed, high pressure, liquid hydrogen turbopump was retrofitted with hybrid bearings to investigate the application of the test bearings to an actual turbopump and to demonstrate the feasibility of using the bearings. The MK48 is a three-stage centrifugal LH_2 turbopump with a design point discharge pressure of 3140 N/cm^2 (4560 psia) and a mass flow rate of 2.74 kg/s (6.04 lb/sec) at 9948 rad/s (95 000 rpm). The turbopump is fully described in reference 1. The MK48 rotor is shown in Figure 2(b). The original duplex sets of conventional ball bearings were replaced with hybrid bearings at both the pump and turbine bearing positions. During

steady-state operation of the pump, axial loads are carried by a balance piston on the back of the third stage impeller. During transients, the axial loads are carried by the turbine end ball bearings and transferred through rub rings on the ends of the turbine end journal bearing. Tests were conducted with the individual bearing flows supplied from either controlled external pressure sources or from internal (pump) sources. For the internal flow tests, the pump end bearing was supplied from a tap off at the first stage impeller discharge and the turbine bearing was supplied from the pump discharge duct.

Instrumentation

Conventional measurements of temperatures, pressure, and flow rates were taken as required. Two of the hydrostatic fluid film pockets contained pressure taps which allowed the fluid film pressure drop from the pocket to the bearing sump to be measured. One of the instrumented pockets was on the vertical center line of the bearing approximately in line with the applied load. The second instrumented pocket was located 90° from the first. The radial deflections of the rotating journals under known applied loads were measured. The bearing deflections were measured by two orthogonally mounted eddy current proximity probes that penetrated the test rig and viewed the rotating journal. An in-place continuous calibration at liquid hydrogen temperature was obtained for every revolution by means of a measured notch in the journal that passed under each probe every revolution. Using this system, journal deflections as small as 0.0025 mm (0.0001 in.) could be detected and measured. The combination of measured radial load and radial deflection allowed the bearing direct stiffness to be determined.

PROCEDURE

After the rotor was balanced, the tester (or pump) was assembled in a clean room and sealed to prevent moisture condensation until it could be installed in the test facility. As part of each test day, the installed test rig and all of the associated liquid hydrogen systems were vacuum dried and purged with inert gaseous helium to exclude any condensible gases. The final vacuum was broken with hydrogen gas and precooling begun immediately.

Steady-State Tests With NASA Tester

During the steady state bearing characterization tests, the liquid hydrogen flow to the hybrid and axial thrust bearings was established prior to shaft rotation. Once the components were prechilled to steady state conditions the shaft was accelerated to the selected test speed. Simultaneously, the liquid hydrogen drain and the hydrostatic bearing supply pressures were ramped up to the selected pressures. Ramp generators allowed both the ramp rates and the ramp end points (steady state operating conditions) to be set independently. Once all test conditions were established, the radial load was gradually applied. By adding and then removing the radial load the deflection of the hydrostatic film due to the load was noted and the direct stiffness of the film determined. In a single long test, the direct stiffness and other bearing characteristics could be measured at several combinations of pressure drop and shaft speed. For all of these tests the journal and the shaft rotated as a solid body (i.e., virtually no ball rolling).

Cyclic Tests With NASA Tester

To properly simulate the turbopump internal fluid supply and environment during the shaft speed transients with the bearing tester it was necessary to control bearing supply pressure and radial shaft load to be proportional to shaft speed squared. The selected acceleration rate and the radial shaft load were typical of high speed, high pressure turbopumps of the size appropriate to the bearings. The bearing supply pressure and maximum speeds for the cyclic tests were selected to avoid operation at any of the tester critical speeds. Prior to the cyclic test series the tester was cleaned and assembled with new ball bearings.

For the cyclic tests the rotor shaft was accelerated to 5200 rad/s (50 000 rpm) in 1.8 seconds. The liquid hydrogen pressure to the hybrid bearings and the radial load were initially zero although the bearings were bathed in LH_2. During the acceleration, both were increased proportional to shaft speed squared to maximum values of 179 N/cm^2 (260 psid) and 111 N (25 lbf), respectively, for a shaft speed of 5200 rad/s (50 000 rpm). The liquid hydrogen drain pressure was also controlled proportional to shaft speed to a maximum value of 55 N/cm^2 (80 psia). Once the journal speed, which characteristically lagged the shaft speed (fig. 3), reached 5200 rad/s (50 000 rpm) the shaft was decelerated to zero speed using the same control criteria. This constituted one start/stop cycle. These cycles were repeated for a total of 337 cycles at which time the tester was disassembled.

Turbopump Application Tests

A similar test procedure was used to demonstrate the application of hybrid bearings in an actual turbopump. Eddy current probes were used to measure journal speeds, axial motion and radial motion. No direct stiffness measurements were made because the magnitude of the radial loads could not be measured. The initial turbopump tests were run with the bearing flows supplied from an external facility source. The pump end and turbine end bearing supply pressures were controlled independently and the individual flow rate measured. During these tests a wide range of speeds and supply pressures were achieved. The test facility was equipped with controllers which could simulate pump fed supply pressures to the bearings. In the final series, tests were made with both the hybrid bearing flows supplied from within the turbopump. Individual bearing flow rates were also measured in these tests by routing the tapped off pump source flows through flow measuring orifices prior to routing the flow into the bearing supply line.

RESULTS AND DISCUSSIONS

Experimental results are presented from tests conducted under simulated conditions in a bearing tester and in an actual turbopump environment. Experimental values of direct stiffness, flow rates, and pressure drops for the hydrostatic film portion of the bearing are presented for a wide range of test conditions obtained using the bearing tester data. These results are compared to theoretical values. Typical transient behavior for a long series of cyclic life tests using the bearing tester is also shown. Data are presented for turbopump tests using the hybrid bearings at both rotor bearing locations. Steady state and transient operation over a wide range of speed and supply pressure is described and the integration of the hybrid bearing into a liquid hydrogen turbopump is discussed.

Direct Stiffness

Because of the extremely low viscosity of liquid hydrogen the fluid film acts nearly as a pure hydrostatic bearing. The stiffness of a hydrostatic bearing is determined by (1) bearing length, (2) bearing diameter, (3) radial clearance, and (4) the pressure drop across the bearing. The measured stiffness of the hybrid bearing as a function of speed is shown in Figure 4 for constant pressure drop across the bearings. The variation in stiffness with speed at a constant pressure drop is due to changes in the radial clearance caused by centrifugal growth of the journal as shown in Figure 5. The stiffness was determined by measuring the radial deflection of the rotating journal for a known amount of applied non-rotating radial load.

The first critical speed for the bearing tester as a function of stiffness was determined by observing the amplitude of the shaft orbit. The amplitude of the shaft orbit begins to increase as the resonance is approached from above or from below. The maximum amplitude occurs at resonance and is shown by the solid curve in Figure 4. Steady state operation was possible at resonance with the hybrid bearings. Damping was not measured; however, it was apparent that the hydrostatic film provided sufficient damping to allow operation in a resonance condition. Another indication of the high degree of damping was the wide dynamic response spectrum. The broken lines on either side of the critical speed curve in Figure 4 show the limits of the response spectrum as determined by increased orbit amplitude.

A comparison of measured and predicted stiffness for the hybrid bearing is shown in Figure 6. In this figure, stiffness is presented as a dimensionless stiffness parameter, $\overline{K}$, which generalizes the physical variables of bearing length, L, and diameter, D; the total pressure drop across the bearing, DPT; and the direct stiffness, K. Dimensionless stiffness is shown as a function of pressure ratio. The pressure ratio is defined as the film presssure drop, DPF, measured from the pocket recess to the bearing sump, divided by the total pressure drop, DPT measured from the bearing supply upstream of the control orifice to the bearing sump. This pressure ratio, $\overline{PR}$, is nearly constant over a range of flow rates for a fixed geometry hydrostatic bearing. But, for the bearing tested $\overline{PR}$ increased with speed because the clearance decreased with speed. $\overline{PR}$ as a function of speed is shown in Figure 7.

Theoretical studies of hydrostatic bearings such as Ref. 1 have shown that $\overline{K}$ is maximum when $\overline{PR}$ is approximately 0.55. Using the parametric design curves in Ref. 2, a predicted $\overline{K}$ at $\overline{PR}$ of 0.55 was determined for the test bearing. This predicted $\overline{K}$ along with several experimental points are shown as a function of $\overline{PR}$ in Figure 6. It can be seen that the measured stiffness was approximately 50 percent higher than predicted. Although there are limited data at high $\overline{PR}$ it appears that the maximum $\overline{K}$ occurs at $\overline{PR}$ of 0.55 as predicted.

Experimentally determined stiffness is higher than predicted using the methods of Ref. 2. Under predicting stiffness by 50 percent could produce significant errors in any dynamic analysis results which used the stiffness predictions as input.

Flow Rate

The experimental flow rates for the hydrostatic bearing were found to be lower than predicted. A simplified way to present the difference between theoretical and experimental data is to consider a fluid film flow resistance coefficient, R_f, defined as film pressure drop divided by flow rate

squared. Predicted values of R_f as a function of radial film clearance for the test bearing were presented in Reference 3 and are shown in Figure 8. These predictions include the effects of rotation, turbulence, and inertia at the edges of the recess pockets as determined using the methods described in references 2 and 4. Also shown in Figure 8 are values of R_f computed from the experimental data. The experimental film pressure drop was measured 90° from the load line and without any applied radial load, i.e., with the journal nearly concentric. The variation in clearance, c, for the experimental data was due to the centrifugal growth of the rotating journal. At a clearance of 0.066 mm (0.00260 in.), which corresponds to zero speed (rotation), the experimental R_f is greater than the predicted value. As clearance decreased (speed increased) the difference between the experimental and the predicted value increases. Using the respective R_f values from Figure 8, the ratio of experimental to predicted flow rate, FLOR, is shown as a function of clearance in Figure 9 and as a function of speed in Figure 10. At zero speed the experimental flow rate is approximately 80 percent of the predicted value. The percentage of the experimental to predicted value decreases with increasing speed. At 8400 rad/s (80 000 rpm), the experimental flow rate is approximately 40 percent of the predicted value. In summary, the state-of-the-art prediction method does not predict any significant effect of journal rotation on the flow. Yet, the experimental data indicate that the speed does have a significant effect.

One explanation for this discrepancy between the measured and predicted flow rates has been offered in Reference 3 where an "effective roughness" has been used in an empirical prediction of flow rate using the methods of References 5 and 6. The surfaces of the actual hardware were very smooth and, therefore, no roughness effect was predicted. But, when an "effective roughness," approximately four times the actual value, was applied to the present data the measured flow rates were within 15 percent of the corresponding predicted values over a wide range of speed and pressure drop. In the empirical flow prediction model increasing the roughness reduces the flow rate and increases the sensitivity to speed.

Cyclic Life

In addition to the steady state tests, 337 cyclic tests were made to determine the life characteristics of the hybrid bearing under simulated turbopump transient operating conditions No hardware failures occurred and, therefore, no life limit was determined.. There were no intermediate tear downs of the hardware during the cyclic testing. Typical start/stop transients are shown for a single test cycle in Figures 11 to 13. The maximum values and the shaft acceleration rates were the same for all of the 337 cycles. The shaft acceleration rate was 2900 rad/s^2 (28 000 rpm/sec) to a maximum speed of 5200 rad/s (50 000 rpm). The maximum radial load and total bearing pressure drop were 200 N (45 lbf) and 172 N/cm^2 (250 psid), respectively. Series of up to 26 cycles were made in a continuous test string. The number of cycles in a continuous string was limited by the data computer storage.

As shown in Figure 11 the journal speed lags the shaft speed during the start and also sometimes during the stop transients. Journal speed lag during a stop transient means that the ball bearings can sometimes actually reverse direction. Bearing pressure drops and the sump pressure are shown in Figure 12 for typical transients. The total bearing pressure drop and the sump pressure were controlled in these tests to increase and decrease proportional to

shaft speed squared. The fluid film pressure drops increase as the journal speed increases due to the decreasing clearance with speed. The eccentricity caused by the applied radial load can be seen by comparing the two fluid film pressure drops shown in Figure 12. The lower presssure differential is measured in the load line at the top of the journal. The higher differential pressure is measured 90° to the load and is only slightly different from the concentric value. The combination of the rapid increase in total bearing pressure drop and the slower increase in film pressure drop (increasing journal speed) causes flow rate to reach a maximum value early in the transient and then approach a lower steady state value as the journal speed approaches the shaft speed (Fig. 13).

The degree to which the journal speed lags the shaft speed is shown to be a function of the shaft acceleration rate in Figure 14. For comparison the solid symbol shown is for a test where the bearing flow was established prior to the start of rotation. The dependence of the journal speed lag on the shaft acceleration rate indicates that the lag is more an inertia effect than rubbing of the journal. High resolution journal displacement and rotation data indicate that the journal lifted before there was rotation and, therefore, there was virtually no rubbing during the acceleration transients. Observation of the journal speed during the stop transients, however, shows some quick stops indicating rubbing of the journal. Sometimes the stops were relatively gentle and other times very sudden from speeds as high as 1000 rad/s (10 000 rpm). The resultant wear associated with the sudden stops appears to be negligible probably because of the low inertia required to decelerate the rather light weight journal.

Although no life limit was determined, the 337 cycles demonstrated exceeds the reasonable expected life of conventional ball bearings under similar operating conditions. Post test inspection indicated that there had been rubbing of the journal but even with this abuse the bearing continued to operate. The stop transients appear to be more severe than the start transients. One possible way to reduce the severity of the stop transient is to provide a check valve, plenum, and orifice type system to prolong the bleed down of the film flow, and keep the bearing lifted to lower speeds.

Turbopump Application

The MK48 liquid hydrogen turbopump was used as a test bed to demonstrate the feasibility of application of hybrid bearings in a full turbopump assembly. The design point speed of the MK48 is 9900 rad/s (95 000 rpm). The pump had been operated successfully over a wide range of speeds using conventional ball bearings (ref. 1). In the present test series, fifteen tests were made with the MK48 turbopump retrofitted with hybrid bearings. A total of 1261 seconds of operation at speeds up to 8200 rad/s (88 000 rpm) and with shaft acceleration rates of up to 5400 rad/s^2 (52 000 rpm/sec) were achieved with no damage to the bearings (ref. 3).

In the design of hybrid bearings for the pump, consideration had to be given to the available supply pressure and sump pressures to attain the proper bearing stiffness. The sump pressures at the two bearing locations were fixed by the pump design, but there were several choices for the supply pressure depending on the tap off location chosen. Pressures at several locations in the pump are shown in Figure 15 as a function of speed. The first stage impeller discharge (655 N/cm^2 (950 psia)) and the pump discharge (2413 N/cm^2 (3500 psia)) were selected to supply pressure to the pump end and turbine end bearings, respectively.

In the initial tests, the hybrid bearing flow was supplied from an external facility source. This was done to have better control of the bearing stiffness during the pump accelerations and also to provide the flexibility to test the bearing over a range of operating conditions. An example of the versatility of the bearing is shown in Figure 16. The numbered points each represent successful steady state operation and show the combinations of speed and supply pressure tested during a single test. The changes in supply pressure represent changes in stiffness. Although, the direct stiffness could not be measured on the turbopump because the applied load was not known, evidence of the change in stiffness can be seen in Figures 17 and 18, where shaft orbit diameters are shown as a function of speed for two different tests. The critical speeds are functions of the bearing stiffness. By changing the bearing pressure drop from 310 to 17 N/cm^2 (450 to 25 psid), the first critical was shifted from 4000 rad/s (38 000 rpm, Fig. 16) to 1000 rad/s (10 000 rpm, Fig. 18).

For the final four tests with the turbopump the bearings were supplied from the internal pump sources as previously described. During steady state operation the pump end bearing rotated synchronously with the shaft up to speeds of 7300 rad/s (70 000 rpm). During the rapid shaft accelrations the pump end journal lagged the shaft speed similarly to the NASA tester data (Fig. 11). The measured test flow rates were 30 to 50 percent lower than predicted. The difference between the measured and predicted values increased with increasing speed. These flow rate results are also quite consistent with the NASA tester data. The turbopump performance data do show a performance penalty for using the hydrostatic bearing due to the recirculation of the bearing flow, but the penalty is not great. The use of hydrostatic bearings will allow significant increases in speed which will produce increases in turbopump efficiency. The increase in efficiency will pay back the performance loss due to the increased recirculation flow.

For the simulated pump internally supplied operation, the hydrostatic bearing pressure increased as a function of pump speed (Fig. 15). Variability in control of supply presssure (and bearing stiffness) provided opportunities for control of the shaft dynamics during transients. This allowed effective control of the crossing of rotor natural frequencies. If the rotor design and rotordynamic controls were developed properly so that the rotor natural frequency parallels the shaft speed in the operating range, but without matching it, the critical speed could be avoided. Typical examples of the predicted rotor natural frequency corresponding to two supply pressure profiles as a function of speed are given in Figure 19. The long dashed curves show how the first four rotor natural frequencies tend to parallel the shaft speed in a system where the bearing supply pressure increases as a function of speed squared. The short dashed curves show how the rotor natural frequencies can be controlled by scheduling the bearing supply pressure. For the case shown, the bearing supply pressure was held constant above 6800 rad/s (65 000 rpm).

Another concern in using hydrostatic bearings is the potential for subsynchronous rotor instabilities. If the dissapative forces acting on the rotor do not exceed the excitation forces, the rotor will respond to the excitation with unbounded amplitude growth until limited by rubbing. The additional source of excitation not found in conventional ball bearings is the rotating fluid film acting on the journal and creating cross-coupled forces. The response of a rotor to an excitation is a function of both the direct and the cross-coupled stiffness and damping. For the hydrostatic bearing, as the direct stiffness is increased by increasing the bearing supply pressure, the cross-coupled stiffness also increases. But, because the cross-coupled terms

increase faster than the direct terms, there is a resultant decrease in the stability threshold of the rotor. The amplitude growth of a rotor excusion in response to excitation is described by the expression $e^{\lambda t}$, where t is time. If λ is negative, the amplitude will decay and the rotor is stable. The response parameter, λ, is shown as a function of speed in Figure 20 for different schedules of supply pressure. The most stable case is for the lowest supply pressure.

The proper rotordynamic design of a given turbopump is highly dependent on the accuracy of prediction of direct and cross-coupled stiffness and damping coefficients. Bearing test results presented earlier indicate that experimental stiffness is approximately 50 percent greater than predicted using the present analytical methods available.

Integration of the hybrid bearings into the existing turbopump was not completely succesful. The added radial clearances created by the use of the hydrostatic bearing clearances caused slight rubbing of the high pressure balance piston orifice. The rubbing of the balance piston orifice could have been prevented with a simple redesign, but this modification was beyond the scope of the effort to retrofit an existing turbopump. The balance piston, which was positioned on the rear of the third impeller stage, is used to provide axial thrust control and axial positioning of the shaft. The radial rubbing and wear caused the shaft axial position to move from the desired design point. The turbine end hybrid bearing journal was designed with close clearance end play in order to accommodate transient axial thrust at startup and shutdown. The axial repositioning of the shaft due to high pressure orifice rubbing caused the turbine end journal to have inadquate end play during steady state operation and the journal was prevented from rotating freely. The effect of zero journal speed (no rotation) changed the expected clearance and resultant stiffness and damping coefficients. This resulted in lower critical speeds and increased rotordynamic vibration amplitudes at high shaft speeds. The pump-end hybrid bearing had no end play restrictions and operated successfully providing excellent data from the test program. Due to the turbine end journal problems, direct correlation of predicted rotordynamic characteristics to the test results were not possible.

The data in Figures 17 and 18 show that vibration levels were increasing steadily as speed was increased. The shaft orbit diameters measured are not absolute in value, but approximate. The measurements are located just outboard of the pump end bearing. As the speed increased to above 7300 rad/s (70 000 rpm), the amplitudes indicated provide the energy to load the hydrostatic journal to the point of slight radial contact and, therefore, limited the hybrid bearing tracking of shaft speed. Increased stiffness and/or reduced vibration amplitudes would have allowed the hybrid bearing to operate synchronously at higher shaft speeds than those obtained. Post test inspection of the hybrid bearings indicate that the bearings are extremely rugged. There were some streaks on the journal outside diameter and on the hydrostatic bearing inside diameter apparently from rubbing during the transients. There were no significant grooves or build up of silver. There was virtually no wear on the ball bearings and no indication of imminent failure.

Hybrid bearings are feasible for use in high speed turbopump applications. The tests have shown very satisfactory operation in startup and acceleration as well as steady state speeds up to 7300 rad/s (70 000 rpm). One of the major design problems associated with the hybrid bearing related to high speed turbomachinery is the requirement for free end play so as not to interfere with rotation of the hydrostatic journal. To ensure end play, it is preferred that the bearing not have responsibility to control the transient axial

thrust loads. This problem can be overcome with the inclusion of a transient thrust bearing or other transient control methods.

SUMMARY OF RESULTS

Two different experimental programs were conducted to investigate the characteristics of a hybrid (hydrostatic/ball) bearing operating in liquid hydrogen. The same bearing design was used in both programs. Analytical predictions were made of the bearing characteristics and are compared with the experimental results where possible. The first program used a bearing tester to determine the steady state, transient, and cyclic life characteristics of the bearing over a wide range of operating conditions. The second program demonstrated the feasibility of applying hybrid bearings to an existing high speed turbopump by retrofitting and then testing the MK48 liquid hydrogen turbopump with the bearings. The following results were obtained:

1. No failures occurred during 337 start/stop cycles under simulated turbopump operating conditions and consequently, no life limit was determined.
2. Hybrid bearings are feasible for use in high speed turbopump applications. The tests have shown satisfactory operation in startup and acceleration as well as steady state operation up to 7300 rad/s (70 000 rpm).
3. The measured direct stiffness of the hydrostatic bearing was approximately 50 percent greater than predicted.
4. The measured flow rates for the hydrostatic bearing were lower than predicted. The measured flow rate was approximately 80 percent of the predicted value at zero speed and 40 percent at 8400 rad/s (80 000 rpm). The apparent effect of speed on flow rate was an unexpected result for the range of test conditions.
5. Observation of the journal speed transients indicate that the most severe rub condition is during shutdown. The journal sometimes made quick stops from speeds as high as 1000 rad/s (10 000 rpm). However, the test results indicate that the bearing is extremely rugged and the rubbing did not cause disfunction of the bearing probably because of the low inertia associated with decelerating the rather light weight journal.
6. Hydrostatic bearing pressure and flow, when internally supplied by the pump, increased with shaft speed. As a result, the bearing stiffness and critical speeds also increase with shaft speed. Bearing designs are, therefore, possible which can be used to control or to avoid critical speeds during the transients.
7. A major inherent design problem associated with hybrid bearings in high speed turbopump applications is the requirement for free end play so as not to interfere with rotation of the hydrostatic journal. Design alternatives for transient axial thrust control appear possible to solve the problem.
8. Successful steady state operation of the rotor at critical speeds indicates that the hybrid bearings have significantly more damping than conventional ball bearings.

REFERENCES

1. Csomor, A. and Warren, D. J., "Final Report-Small High-Pressure Liquid Hydrogen Turbopump," Rocketdyne, Canoga Park, CA, RI/RD79-322, May 1980. (NASA CR-159821.

2. Young, W. E. and Reddecliff, J. M., "Investigation of Hydrostatic Bearings for Use in High Pressure Cryogenic Turbopumps," Pratt a Whitney Aircraft, PWA-FR-2343, May 1967. (AFRPL-TR-67-130).
3. Nielson, C. E., "Final Report-Hybrid Hydrostatic/Ball Bearings in High-Speed Turbomachinery," Rocketdyne Division, Canoga Park, CA. RI/RD83-104, Jan. 1983. (NASA CR-168124).
4. Elrod, H. G., and Ng, C. W., "A Theory for Turbulent Fluid Films and its Application to Bearings," ASME Paper 66-LUB-12, Oct. 1966.
5. Yamada, Y., "Resistance of a Flow Through an Annulus with an Inner Rotating Cylinder," Bulletin of JSME, Vol. 5, No. 18, pp. 302-310, 1962.
6. Yamada, Y., "On the Pressure Loss of Flow Between Rotating Co-Axial Cylinders with Rectangular Grooves," Bulletin of JSME, Vol. 5, No. 20, pp. 642-651, 1962.

TABLE I. - HYDROSTATIC BEARING

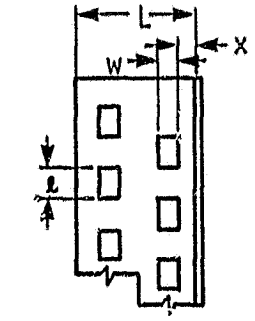

DEVELOPED BEARING SURFACE

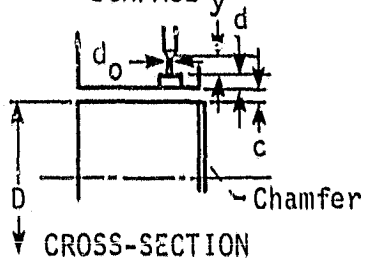

CROSS-SECTION

		cm	in.
Journal outside diameter	D	4.383	1.7255
Radial clearaance	c	See figure 5	
Journal length	L	2.286	.900
Pocket axial length	W	.231	.091
Pocket circumferential length	ℓ	.589	.232
Pocket depth (max)	d	.056	.022
Orifice diameter	do	.066	.026
Orifice length	y	.114	.045
Axial land length	x	.599	.236

Number pockets per row	10
Number rows	2
Journal material	INCO 718 with Thin Dense Chrome Plate
Bearing material	316ss with ED Silver plate

TABLE II. - BALL BEARINGS

	cm	in.
Bearing Bore	2	.7873
Bearing O.D.	3.90	1.5354
Pitch Diameter	2.985	1.175
Ball Diameter	.4763	.1875
Diametral Clearance (unfitted)	.0051	.0020
	.0058	.0023
Ring Width	.998	.393
Race Curvature (percent ball dia.)		
-inner ring	53 percent	
-outer ring	52 percent	
Contact Angle	26°	
Materials		
-Balls, Races	CEVM 440C @Rc 58-62	
-Cage	Armalon	

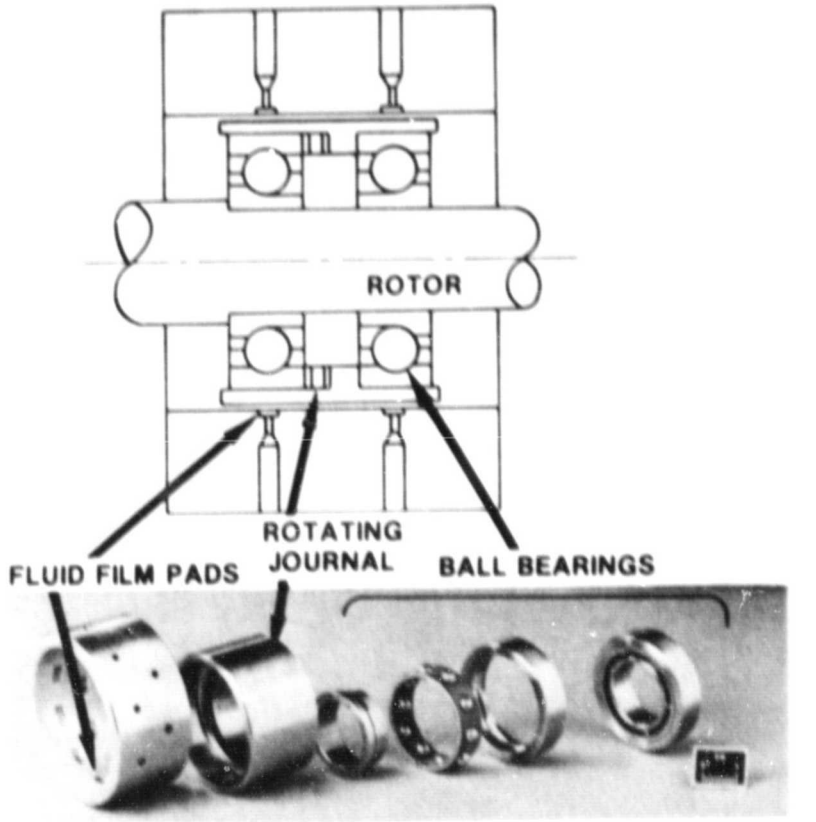

C-81-4304

Figure 1. - Long life hybrid bearing.

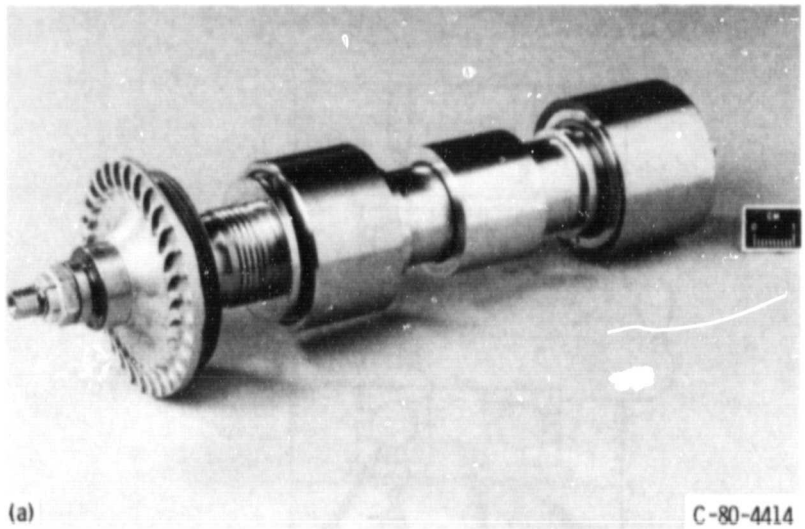

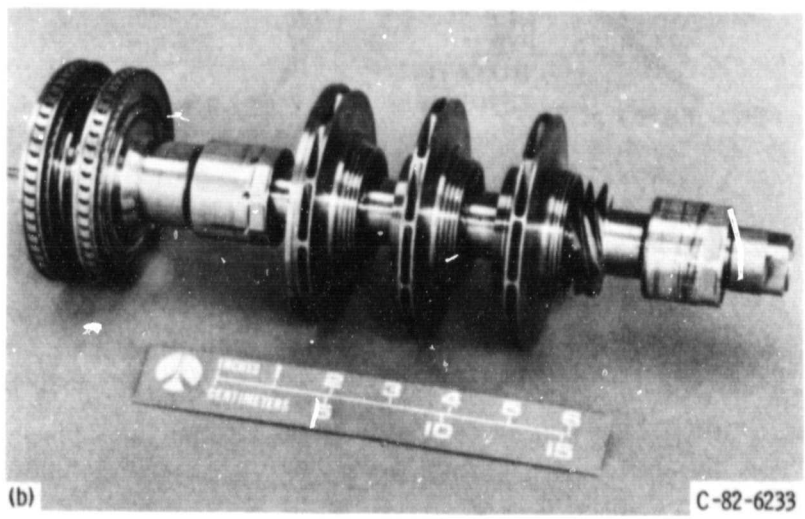

(a) Tester Rotor
(b) MK48 Turbopump Rotor
Figure 2. - Bearing test rotors.

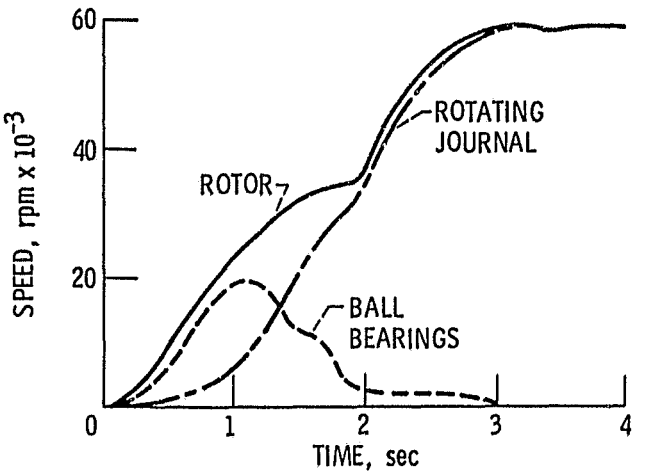

Figure 3. - Hybrid bearing acceleration characteristics.

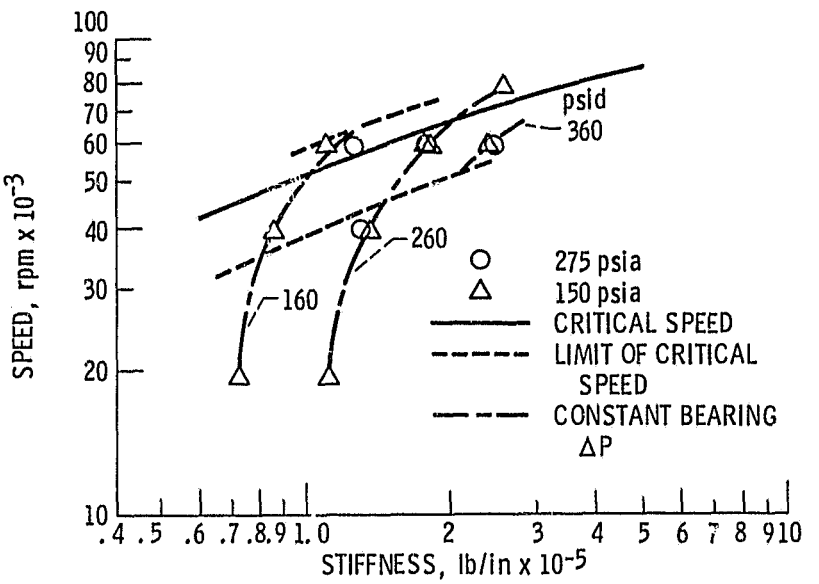

Figure 4. - Hybrid bearing direct stiffness as a function of speed and pressure drop.

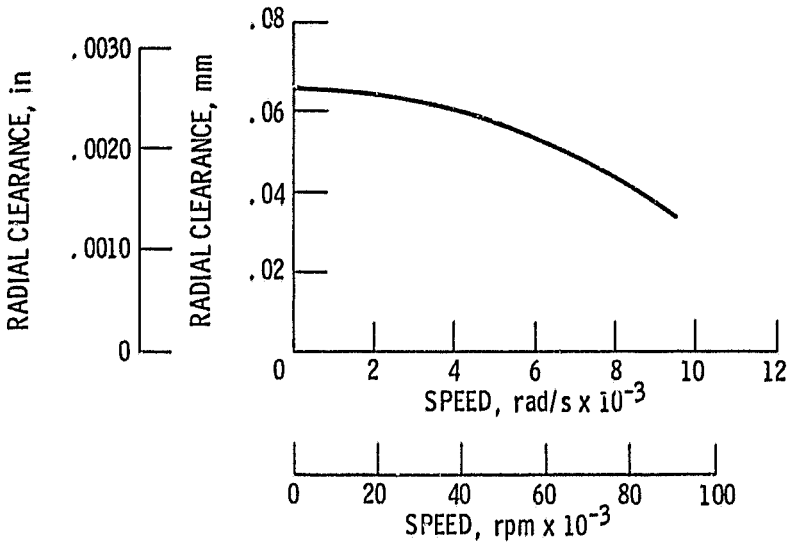

Figure 5. - Computed radial clearance vs journal speed.

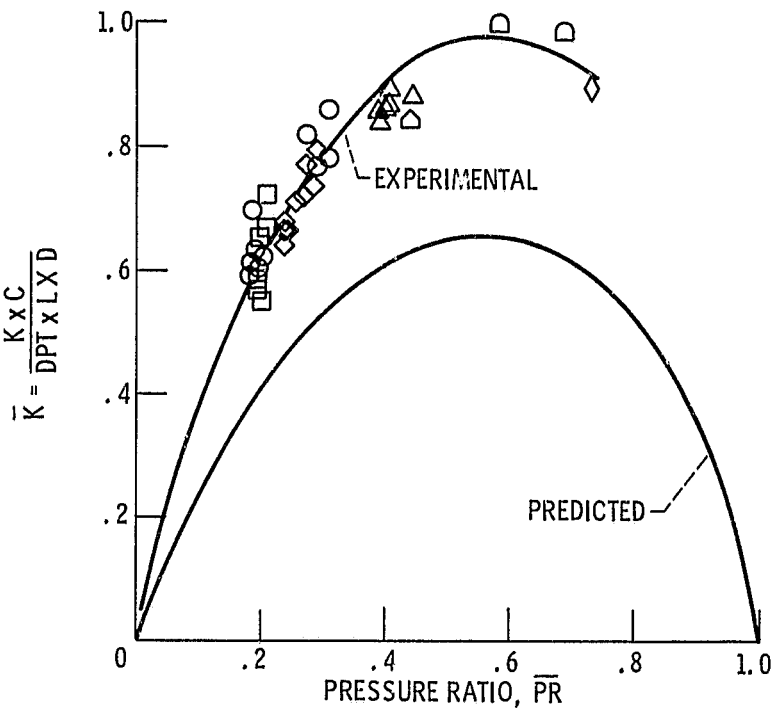

Figure 6. - Dimensionless stiffness as a function of pressure ratio.

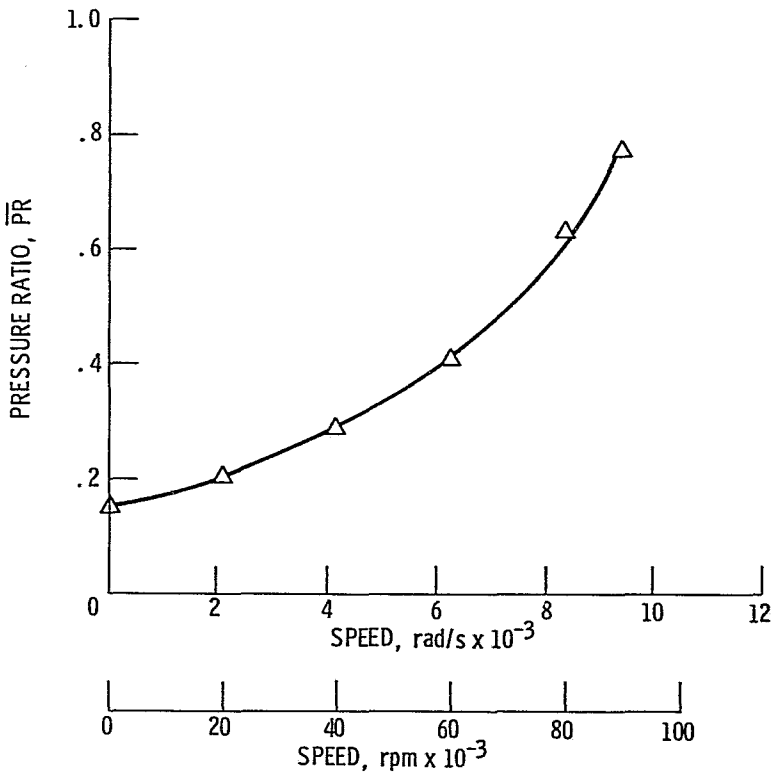

Figure 7. - Effect of speed on pressure ratio.

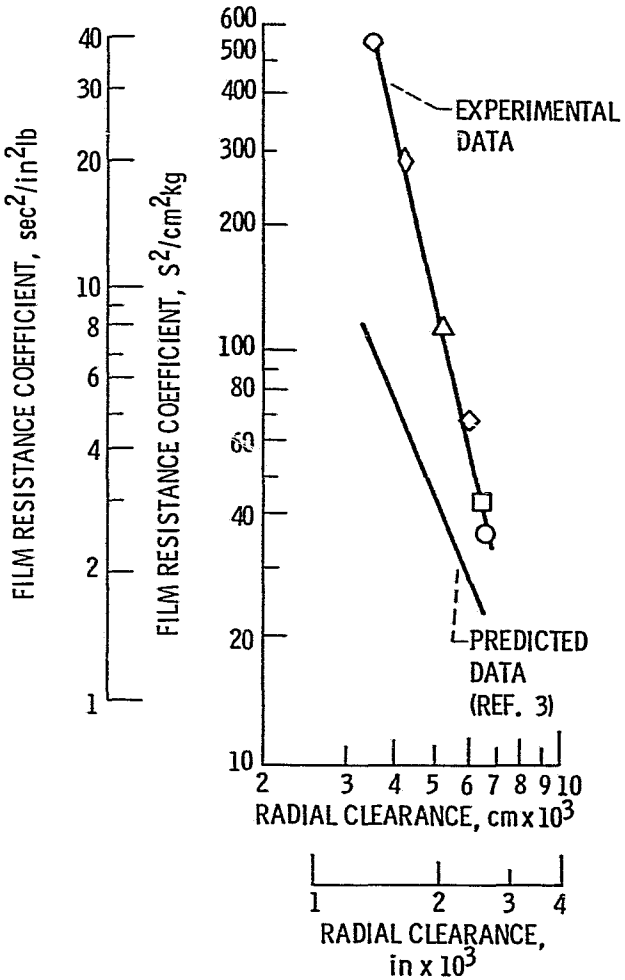

Figure 8. - Effect of radial clearance change due to centrifugal growth on film resistance coefficient.

ORIGINAL PAGE IS
OF POOR QUALITY

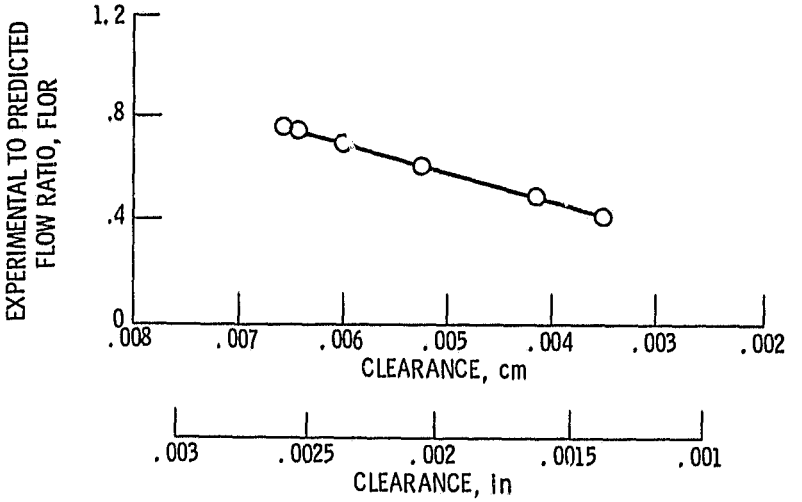

Figure 9. - Effect of clearance change due to circumferential growth on experimental to predicted flow ratio.

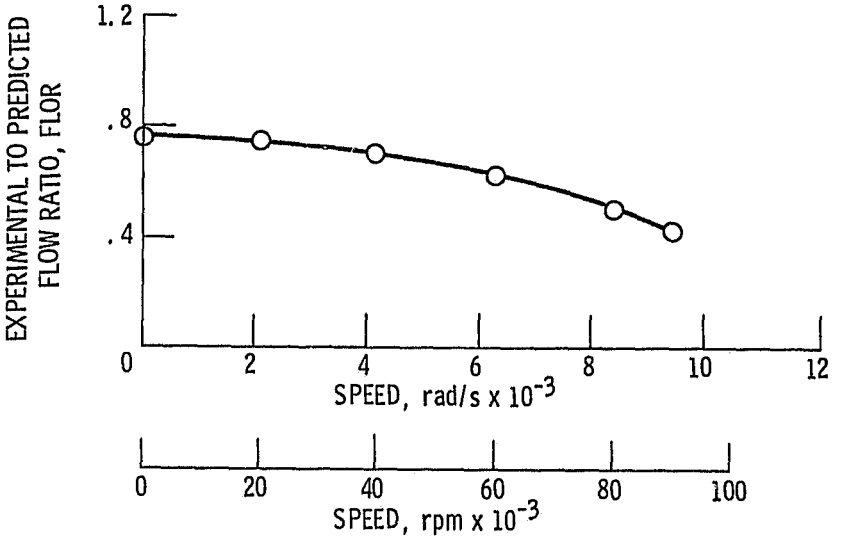

Figure 10. - Effect of speed on experimental to predicted flow ratio.

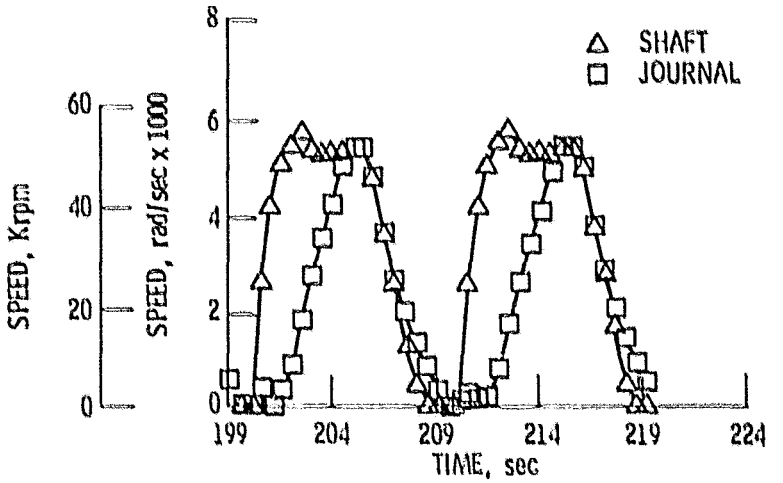

Figure 11. - Shaft and journal speed as a function of time for two cycles of the life test series.

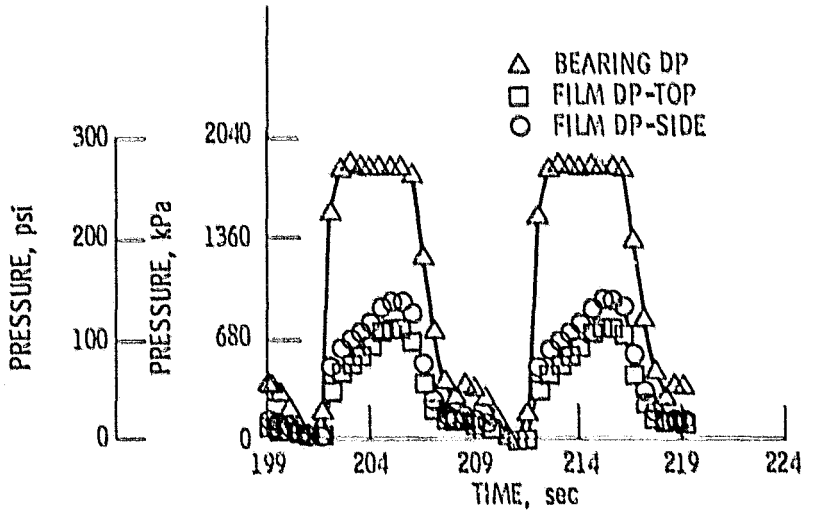

Figure 12. - Bearing pressure drops as a function of time for two cycles of the life test series.

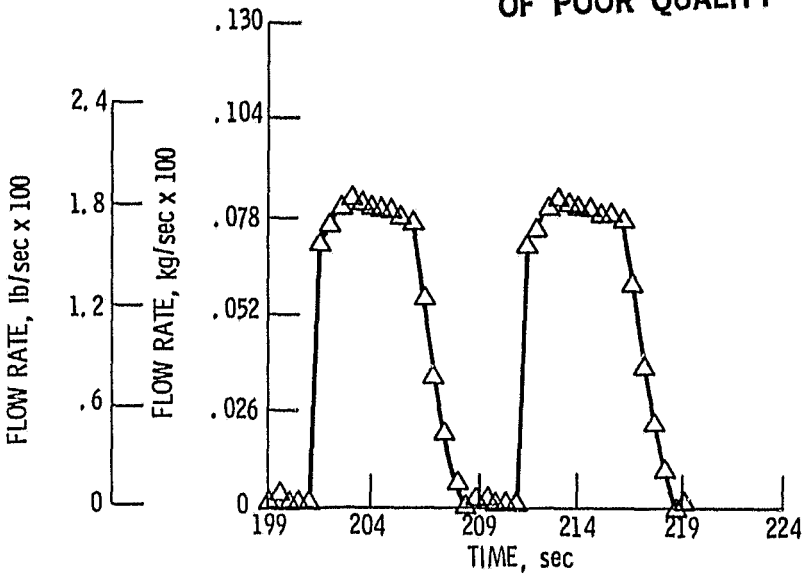

Figure 13. - Bearing flow rate as a function of time for two cycles of the life test series.

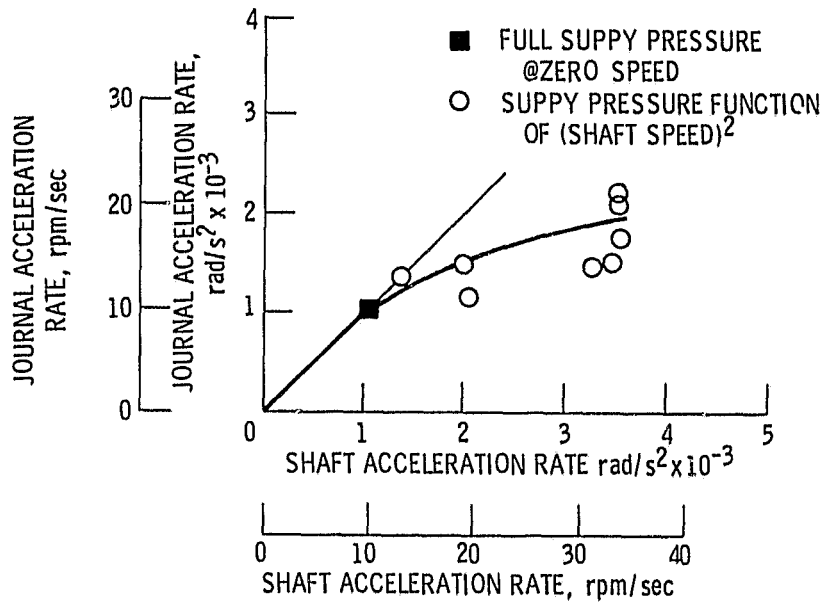

Figure 14. - Comparison of shaft and journal acceleration rates.

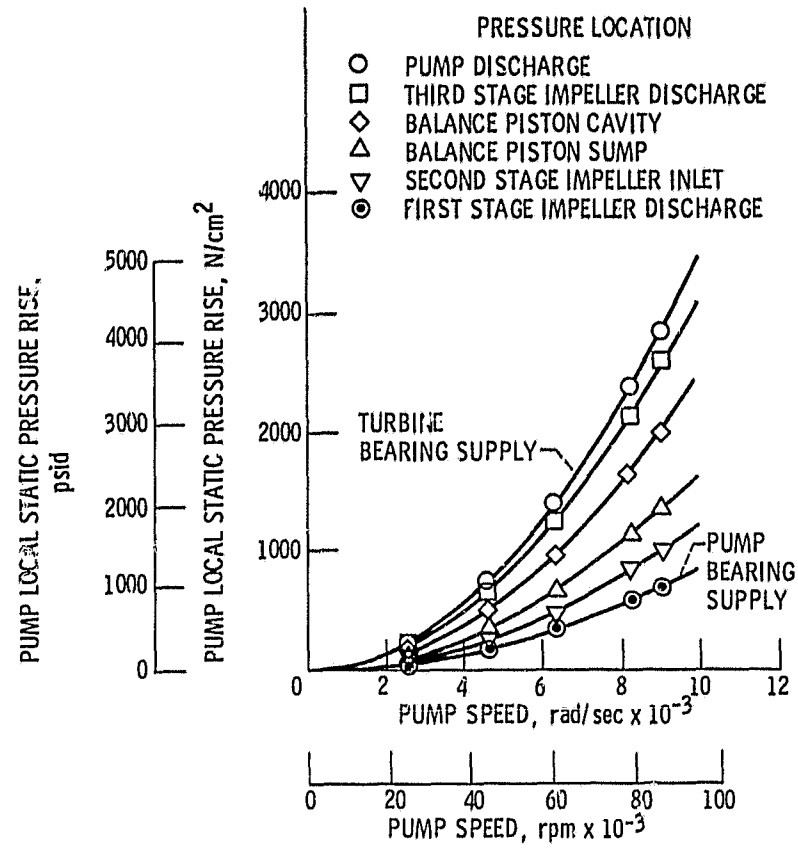

Figure 15. - Mk48 turbopump internal pressures.

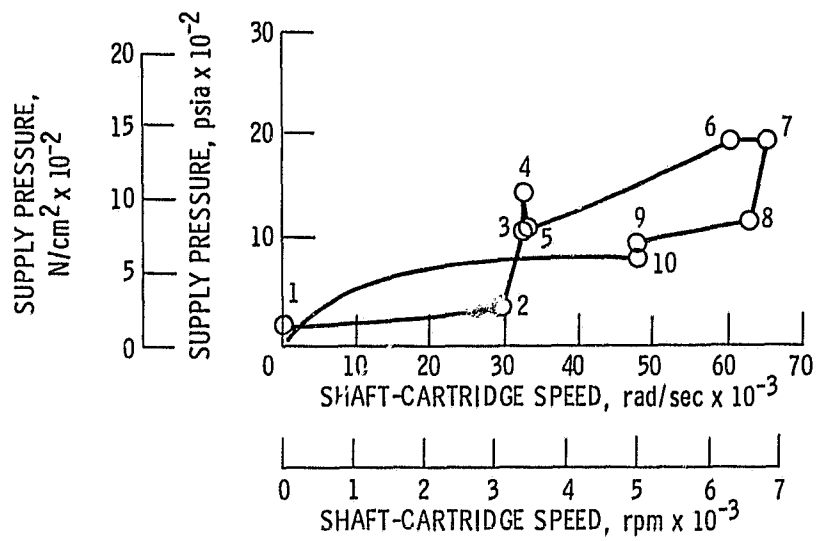

Figure 16. - Versatility of the hybrid bearing as demonstrated by the successful steady state operation at each of the numbered bearing supply pressure and shaft speed data points achieved during a single research test.

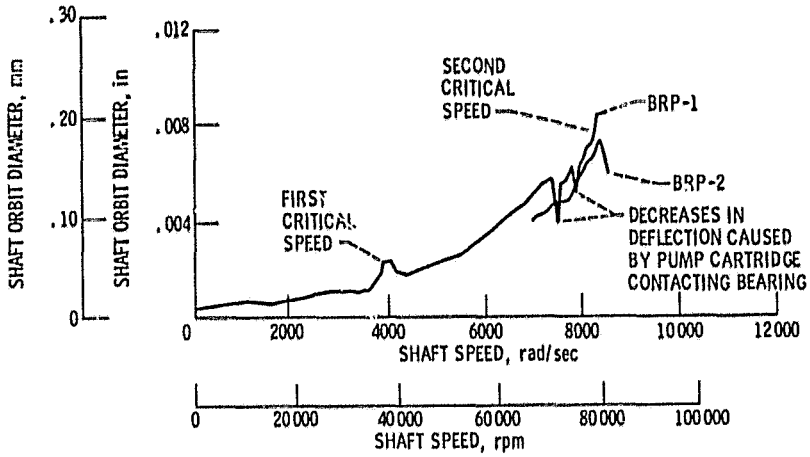

Figure 17. - Shaft orbit characteristics from radial proximeters. DPT = 310 N/cm^2 (450 psid).

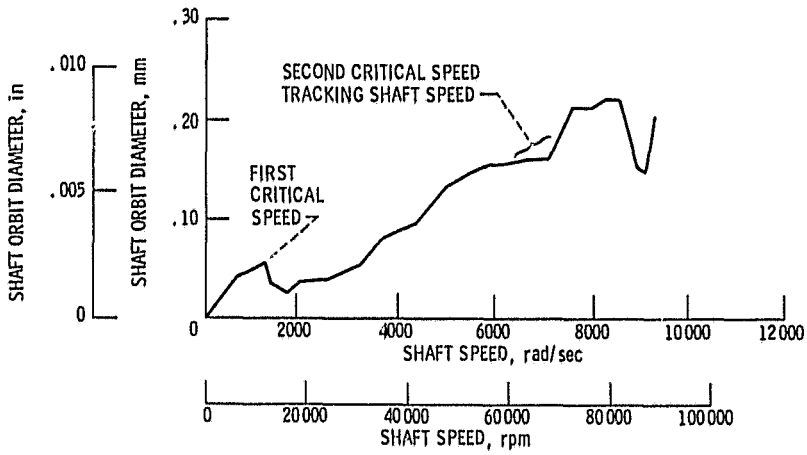

Figure 18. - Shaft orbit characteristics from radial proximeters DPT = 17 N/cm^2 (25 psid).

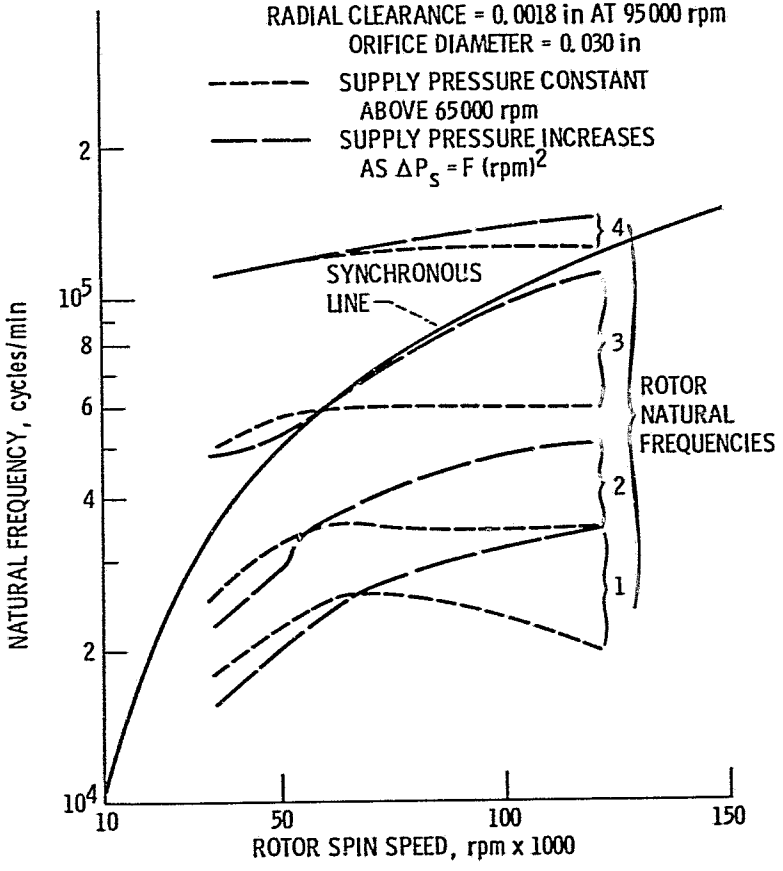

Figure 19. - Hybrid bearing critical speed characteristics for two different supply pressure vs speed schedules.

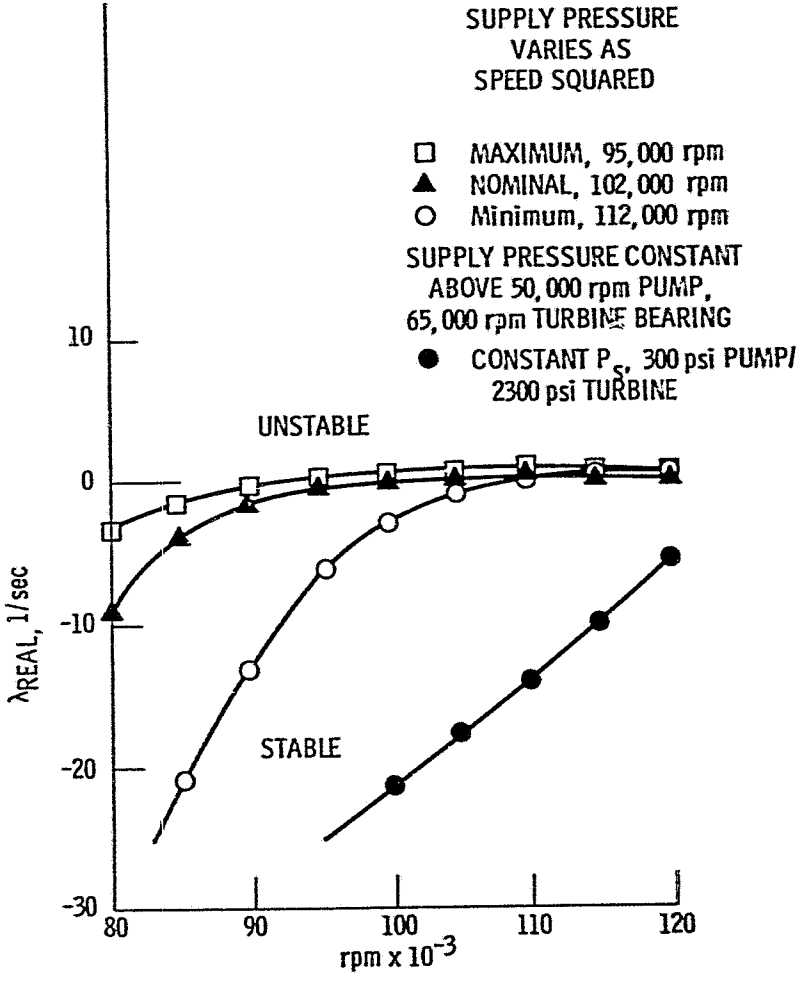

Figure 20. - Effect of supply pressure on hybrid bearing stability. Model assumes no casing damping, no ball bearing damping.